PTEP

Prog. Theor. Exp. Phys. **2021**, 103B05 (16 pages)
DOI: 10.1093/ptep/ptab108

Resolving the Hubble tension in a U(1)$_{L_\mu - L_\tau}$ model with the Majoron

Takeshi Araki[1], Kento Asai[2], Kei Honda[3], Ryuta Kasuya[3], Joe Sato[3], Takashi Shimomura[4], Masaki J. S. Yang[3,*]

[1]*Faculty of Dentistry, Ohu University, 31-1 Sankakudo, Tomita-machi, Koriyama, Fukushima 963–8611, Japan*
[2]*Department of Physics, University of Tokyo, Bunkyo-ku, Tokyo 133–0033, Japan*
[3]*Department of Physics, Saitama University, 255 Shimo-Okubo, Sakura-ku, Saitama 338–8570, Japan*
[4]*Faculty of Education, University of Miyazaki, 1-1 Gakuen-Kibanadai-Nishi, Miyazaki 889–2192, Japan*
*E-mail: yang@krishna.th.phy.saitama-u.ac.jp

Received June 14, 2021; Revised August 6, 2021; Accepted August 6, 2021; Published August 20, 2021

We explore the possibility of resolving the Hubble tension and $(g-2)_\mu$ anomaly simultaneously in a U(1)$_{L_\mu - L_\tau}$ model with Majoron. We only focus on the case where the Majoron ϕ does not exist at the beginning of the universe and is created by neutrino inverse decay $\nu\nu \to \phi$ after electron–positron annihilation. In this case, the contributions of the new gauge boson Z' and the Majoron ϕ to the effective number of neutrino species $N_{\rm eff}$ can be calculated in separate periods. These contributions are labelled $N'_{\rm eff}$ for the U(1)$_{L_\mu - L_\tau}$ gauge boson and $\Delta N'_{\rm eff}$ for the Majoron. The effective number $N_{\rm eff} = N'_{\rm eff} + \Delta N'_{\rm eff}$ is evaluated by the evolution equations of the temperatures and the chemical potentials of light particles in each period. As a result, we find that the heavier Z' mass $m_{Z'}$ results in a smaller $N'_{\rm eff}$ and requires a larger $\Delta N'_{\rm eff}$ to resolve the Hubble tension. Therefore, compared to previous studies, the parameter region where the Hubble tension can be resolved is slightly shifted toward the larger value of $m_{Z'}$.

Subject Index B54, B73, E70

1. Introduction

Recently, a discrepancy has been reported in the values of the Hubble constant H_0 from cosmic microwave background (CMB) measurements [1] and local measurements [2–5]. The inferred value from the Λ cold dark matter (ΛCDM) model with the temperature anisotropy of the CMB measured by Planck [1] is $H_0 = 67.36 \pm 0.54\,\mathrm{km\,s^{-1}\,Mpc^{-1}}$. On the other hand, the local measurements using Cepheids [2,3] and type-Ia supernovae [4] by SH0ES reported larger values: $H_0 = 73.45 \pm 1.66\,\mathrm{km\,s^{-1}\,Mpc^{-1}}$ and $74.03 \pm 1.42\,\mathrm{km\,s^{-1}\,Mpc^{-1}}$, respectively. A similar value of H_0 has also been reported by H0LiCOW from gravitational lensing with late time [5]. These local measurements result in a larger value of H_0 than the CMB measurement.[1] The discrepancy reaches the level of 4–6 σ and is called the Hubble tension.

Although the tension could originate from systematic errors in the measurements [8–10], it would indicate modifications to the standard cosmological model. Several solutions have been proposed in the fields of cosmology and particle physics. One of the approaches to solving the tension is to modify the effective number of neutrino species $N_{\rm eff}$. In Ref. [1], combining the results from the

[1] Local measurements based on the TRGB method [6] and TDCOSMO+SLACS analyses [7] reported values consistent with the CMB results.

Funded by SCOAP[3]

CMB, Cepheids, and others, $N_{\rm eff}$ is derived as 3.27 ± 0.15 at 68% confidence level (C.L.) [11], which implies a difference from the ΛCDM results of $0.2 \lesssim \Delta N_{\rm eff} \lesssim 0.5$ to ameliorate the Hubble tension.[2] Such a difference can be obtained when new interactions with neutrinos exist. In this regard, models with gauged $U(1)_{L_\mu - L_\tau}$ symmetry are very interesting [13–16], under which only mu- and tau-type leptons are charged. It is well known that the long-standing discrepancy of the muon anomalous magnetic moment, $(g-2)_\mu$, can be resolved by the contributions of the new gauge boson Z' with a MeV-scale mass [17–19]. The new interaction also alters the decoupling time of neutrinos from the thermal bath at the early universe. In particular, the decays of Z' to heat neutrinos lead to an increase of $N_{\rm eff}$. In Ref. [20], it was shown that the Hubble tension can be solved simultaneously with the discrepancy of $(g-2)_\mu$.

Other interesting models are those with global lepton number symmetry $U(1)_L$. In the class of the seesaw mechanism, tiny neutrino masses are explained by the heavy Majorana masses of right-handed neutrinos, which can often be generated by the spontaneous breaking of the lepton number symmetry. As a result, a pseudo-Nambu–Goldstone boson, the so-called Majoron, appears in the spectrum [21–24]. From Ref. [25], the decay of the Majoron with a keV-scale mass can increase $\Delta N_{\rm eff}$ by at most 0.11 and hence help to ameliorate the Hubble tension.

Some models with $U(1)_{L_\mu - L_\tau}$ symmetry can reproduce observed neutrino masses and mixing by introducing global $U(1)_L$ symmetry [26]. In such models, the contributions from both the Z' boson and Majoron have to be taken into account by tracking the number and energy densities of light particles in the early universe. In this paper we consider solutions of the Hubble tension in a $U(1)_{L_\mu - L_\tau}$ model with a Majoron by including the contributions of all light particles. For simplicity, we only focus on a case where the Majoron does not exist at the beginning of the universe and is created by $\nu\nu \to \phi$ after $e^\pm$ annihilation. In this case, $N_{\rm eff}$ can be calculated separately from the contribution of the Z' boson and that of ϕ.

The paper is organized as follows. In Sect. 2 we describe the $U(1)_{L_\mu - L_\tau}$ model with the global $U(1)_L$ symmetry. In Sect. 3, we derive the evolution equations of the temperature and chemical potential in the early universe. In Sect. 4 we solve these equations in order to calculate the contribution of Z' and the Majoron to $N_{\rm eff}$ and impose a constraint on the Z' and Majoron parameter space. Finally, we summarize our results in Sect. 5.

2. The $U(1)_{L_\mu - L_\tau}$ model

We consider a $U(1)_{L_\mu - L_\tau}$ model which contains the global $U(1)_L$ symmetry, similarly to Ref. [26]. Such a model can have a keV Majoron as a pseudo-Nambu–Goldstone (pNG) boson originating from the spontaneous symmetry breaking of the $U(1)_L$. In addition, this model has a $U(1)_{L_\mu - L_\tau}$ gauge boson, which can explain the muon anomalous magnetic moment and the IceCube gap of the cosmic neutrino flux if this gauge boson has $\mathcal{O}(10$–$100)$ MeV mass [27–30]. As discussed in Refs. [20,25], these particles can contribute to the expansion history of the early universe and have the possibility of resolving the Hubble tension.

In this section we show the interactions between the electron, neutrino, $U(1)_{L_\mu - L_\tau}$ gauge boson Z', and Majoron ϕ which contribute to the Hubble parameter in the early universe.

[2] We should note that increasing $N_{\rm eff}$ worsens another milder tension relative to σ_8 [11,12], the cosmological parameter concerning the matter density fluctuation amplitude at 8 Mpc scales.

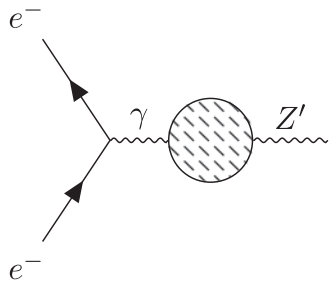

Fig. 1. One-loop diagram which induces an interaction between Z' and electrons.

2.1. *The U(1)$_{L_\mu - L_\tau}$ Lagrangian*

The Lagrangian related to the U(1)$_{L_\mu - L_\tau}$ gauge boson is given by

$$\mathcal{L}_{Z'} = -\frac{1}{4} Z'^{\rho\sigma} Z'_{\rho\sigma} + \frac{1}{2} m_{Z'}^2 Z'^{\rho} Z'_{\rho} + g_{\mu-\tau} Z'_{\rho} J^{\rho}_{\mu-\tau}, \tag{1}$$

where Z' denotes the U(1)$_{L_\mu - L_\tau}$ gauge boson with field strength $Z'_{\rho\sigma} = \partial_\rho Z'_\sigma - \partial_\sigma Z'_\rho$, and $m_{Z'}$ and $g_{\mu-\tau}$ are the U(1)$_{L_\mu - L_\tau}$ gauge boson mass and gauge coupling constant, respectively. $J_{\mu-\tau}$ denotes the $L_\mu - L_\tau$ current and is written as

$$J^{\rho}_{\mu-\tau} = \bar{\mu}\gamma^\rho \mu + \bar{\nu}_\mu \gamma^\rho P_L \nu_\mu - \bar{\tau}\gamma^\rho \tau - \bar{\nu}_\tau \gamma^\rho P_L \nu_\tau. \tag{2}$$

At tree level, the U(1)$_{L_\mu - L_\tau}$ gauge boson interacts only with mu- and tau-type leptons.

2.2. *Effective coupling with electrons*

In this model there can be a gauge kinetic mixing χ between the Z' and the standard model (SM) hypercharge gauge field B: $\mathcal{L}_{\rm mix} = -\frac{\chi}{2} B^{\rho\sigma} Z'_{\rho\sigma}$, where $B_{\mu\nu}$ is the field strength of B. Although we assume that this kinetic mixing vanishes at some high scale for simplicity, non-zero kinetic mixing appears at one-loop level at a low energy scale. This kinetic mixing then induces an interaction between the Z' and electrons through the mixing ϵ of the Z' with the SM photon γ as shown in Fig. 1, and the interaction term is described as

$$\mathcal{L}_{Z'} \supset -\epsilon e Z'_\mu \bar{e}\gamma^\mu e, \tag{3}$$

where ϵ is calculated by

$$\epsilon \simeq \frac{e g_{\mu-\tau}}{12\pi^2} \log \frac{m_\tau^2}{m_\mu^2} \simeq \frac{g_{\mu-\tau}}{70}, \tag{4}$$

with e and m_ℓ the electromagnetic charge and the mass of the charged lepton ℓ.

The partial decay widths of the Z' are given as follows:

$$\Gamma_{Z'\to e^- e^+} = \frac{(\epsilon e)^2 m_{Z'}}{12\pi} \left(1 + \frac{2m_e^2}{m_{Z'}^2}\right) \sqrt{1 - \frac{4m_e^2}{m_{Z'}^2}}, \tag{5}$$

$$\Gamma_{Z'\to \nu_{\mu,\tau}\bar{\nu}_{\mu,\tau}} = \frac{g_{\mu-\tau}^2 m_{Z'}}{24\pi}. \tag{6}$$

Hereafter, we assume that neutrino masses are negligible and taken to be massless. Note that the BABAR experiment excludes the $U(1)_{L_\mu - L_\tau}$ gauge boson with $m_{Z'} > 2m_\mu$ as a solution of the muon anomalous magnetic moment, and thus we assume $m_{Z'} < m_\mu$.

2.3. *Majoron interactions*

The spontaneous breaking of the global $U(1)_L$ symmetry gives rise to a Nambu–Goldstone boson called the Majoron, ϕ. If the global $U(1)_L$ symmetry is slightly broken, then the Majoron has a tiny mass,

$$\mathcal{L}_{\rm mass} = -\frac{1}{2} m_\phi^2 \phi^2. \tag{7}$$

The interaction between the Majoron and neutrinos is described by

$$\mathcal{L}_{\rm int} = g_{\alpha\beta} \bar{\nu}_{L,\alpha} \nu^c_{L,\beta} \phi + h.c., \tag{8}$$

where $g_{\alpha\beta} = g_{\beta\alpha}$ are coupling constants and $\nu^c_{L,\alpha} \equiv (\nu_{L,\alpha})^c = C\bar{\nu}^{\rm T}_{L,\alpha}$ with the charge conjugation matrix C. As we will see later, this interaction can have a significant impact on the early universe.

Using the projection operator as $\nu_{L,\alpha} = P_L \nu_\alpha$, we can rewrite the Lagrangian as

$$\begin{aligned}
\mathcal{L}_{\rm int} &= g_{\alpha\beta} \bar{\nu}_\alpha P_R C \bar{\nu}^{\rm T}_\beta \phi + g^*_{\alpha\beta} \nu^{\rm T}_\alpha C P_L \nu_\beta \phi \\
&= \sum_\alpha g_{\alpha\alpha} \bar{\nu}_\alpha P_R C \bar{\nu}^{\rm T}_\alpha \phi + 2 \sum_{\alpha<\beta} g_{\alpha\beta} \bar{\nu}_\alpha P_R C \bar{\nu}^{\rm T}_\beta \phi \\
&\quad + \sum_\alpha g^*_{\alpha\alpha} \nu^{\rm T}_\alpha C P_L \nu_\alpha \phi + 2 \sum_{\alpha<\beta} g^*_{\alpha\beta} \nu^{\rm T}_\alpha C P_L \nu_\beta \phi.
\end{aligned} \tag{9}$$

In the first equality we used $C(\gamma^5)^{\rm T} = \gamma^5 C$. From the above interactions we obtain the decay width for $\phi \to \nu_\alpha \nu_\beta$, $\phi \to \bar{\nu}_\alpha \bar{\nu}_\beta$ as

$$\Gamma_{\phi \to \nu_\alpha \nu_\beta} = \Gamma_{\phi \to \bar{\nu}_\alpha \bar{\nu}_\beta} = \frac{|g_{\alpha\beta}|^2 m_\phi}{4\pi S_{\alpha\beta}}. \tag{10}$$

Here, $S_{\alpha\beta}$ is a symmetry factor satisfying $S_{\alpha\beta} = 2(\alpha = \beta)$, $S_{\alpha\beta} = 1(\alpha \neq \beta)$.

3. Time evolution equation of temperature and chemical potential

Here we consider the thermodynamics of the early universe in the presence of the new light particles Z' and the the Majoron ϕ. In our study, we assume the following conditions:

(1) For the parameters of the Z', we focus on the region $g_{\mu-\tau} \sim 10^{-4}$–$10^{-3}$ and $m_{Z'} \sim 10\,{\rm MeV}$ to solve the $(g-2)_\mu$ anomaly.
(2) For the Majoron–neutrino couplings given in Eq. (8), we focus on the region $|g_{\alpha\beta}| \lesssim 10^{-7}$ in order to evade the constraints from Big Bang Nucleosynthesis (BBN) [25], KamLAND-Zen [31], and SN1987A [32,33].
(3) We assume that there is no primordial abundance of Majorons, and they are produced after $e^\pm$ annihilation through the inverse decay process $\nu\nu \to \phi$;[3] this assumption corresponds to

[3] The initial condition $n_\phi = 0$ in the early universe where $U(1)_L$ symmetry is restored would be guaranteed as follows. Let S be an original field of the Majoron when the $U(1)_L$ symmetry is unbroken. Here we consider

looking at the parameter region satisfying Eq. (41). The Boltzmann equations with simultaneous contributions from Z' and ϕ are technically difficult to solve. We leave this for future work.

Under condition (2), the scattering and the annihilation processes of Majorons can be neglected, and only the decay and inverse decay of the Majoron, $\phi \leftrightarrow \nu_\alpha \nu_\beta$, $\bar{\nu}_\alpha \bar{\nu}_\beta$, are relevant to our study. Moreover, because of condition (1), the Z' becomes non-relativistic before $e^\pm$ annihilation and decays mainly into neutrinos. On the other hand, from condition (3), Majorons are produced after $e^\pm$ annihilation. Therefore, the thermodynamics of Z' and ϕ can be considered separately, before and after the temperature $T_\gamma \sim 10^{-2}$ MeV at which the electrons and positrons have already annihilated. In the following subsections the evolution equations are derived for each period.

3.1. *Evolution equation before $e^\pm$ annihilation*

We consider the evolution equations for the universe before $e^\pm$ annihilation, at which photons, neutrinos, electrons, and Z' exist. Following previous studies [20,34,35], we make the following approximations in the calculation:

- All the particles follow the thermal equilibrium distribution function.
- In the collision terms we use the Maxwell–Boltzmann statistics.
- Neglect the electron mass m_e in the collision terms for the weak interaction processes.
- Neglect the chemical potentials μ_i for all the particles i.
- The temperatures T_i of a particle i in the same thermal bath are equal; $T_\gamma = T_{e^-}$ and $T_{\nu_\alpha} = T_{Z'} \equiv T_\nu$ for $\alpha = e, \mu, \tau$.

Using these approximations we obtain the evolution equations for the temperatures of photons T_γ and neutrinos T_ν as follows [20]:

$$\frac{dT_\nu}{dt} = -\left(\frac{\partial \rho_\nu}{\partial T_\nu} + \frac{\partial \rho_{Z'}}{\partial T_\nu}\right)^{-1}\left[4H\rho_\nu + 3H(\rho_{Z'} + P_{Z'}) - \frac{\delta \rho_\nu}{\delta t} - \frac{\delta \rho_{Z'}}{\delta t}\right], \tag{11}$$

$$\frac{dT_\gamma}{dt} = -\left(\frac{\partial \rho_\gamma}{\partial T_\gamma} + \frac{\partial \rho_e}{\partial T_\gamma}\right)^{-1}\left[4H\rho_\gamma + 3H(\rho_e + P_e) + \frac{\delta \rho_\nu}{\delta t} + \frac{\delta \rho_{Z'}}{\delta t}\right], \tag{12}$$

with ρ_i and P_i being the energy density and pressure of particle i, respectively, and H the Hubble parameter. Here, the energy transfer rates in Eqs. (11) and (12) are given by

$$\frac{\delta \rho_{Z'}}{\delta t} = \frac{3m_{Z'}^3}{2\pi^2}\left[T_\gamma K_2\left(\frac{m_{Z'}}{T_\gamma}\right) - T_\nu K_2\left(\frac{m_{Z'}}{T_\nu}\right)\right]\Gamma_{Z' \to e^+e^-}, \tag{13}$$

$$\frac{\delta \rho_\nu}{\delta t} = \frac{4G_F^2}{\pi^5}\left[(g_{eL}^2 + g_{eR}^2) + 2(g_{\mu L}^2 + g_{\mu R}^2)\right]F(T_\gamma, T_\nu) + \frac{2(g_{\mu-\tau\epsilon e})^2}{\pi^5 m_{Z'}^4}F(T_\gamma, T_\nu), \tag{14}$$

where G_F is the Fermi coupling constant, K_2 is the modified Bessel function of the second kind, $g_{eL} = 1/2 + s_W^2$, $g_{eR} = s_W^2$, $g_{\mu L} = -1/2 + s_W^2$, and $g_{\mu R} = s_W^2$ with the sine of the Weinberg angle

situations where S develops a vacuum expectation value after weak bosons decouple ($T \ll m_{Z,W}/3$). If the field S is sufficiently heavy and is not created by the decay of other fields, the number density of S in the early universe is negligible. For example, in Ref. [26] the field S_L has a mass of about a TeV that is greater than the masses of the heavy neutrinos, $M_N \sim O(100)$ GeV, and acquires a vacuum expectation value $\sim O(10^{-7})$ GeV. Thus, the initial condition $n_\phi = 0$ is justified.

$s_W \equiv \sin\theta_W$. The function $F(T_1, T_2)$ is defined as

$$F(T_1, T_2) = 32(T_1^9 - T_2^9) + 56T_1^4 T_2^4 (T_1 - T_2). \tag{15}$$

3.2. *Evolution equation after $e^\pm$ annihilation*

We derive the evolution equations for the universe after $e^\pm$ annihilation, at which photons, neutrinos, and the Majoron exist. In analogy with the previous subsection, we make the following assumptions [35]:

- All the particles follow the thermal equilibrium distribution function.
- In the collision terms, we use the Maxwell–Boltzmann statistics.
- $T_{\nu_\alpha} \equiv T_\nu$ and $\mu_{\nu_\alpha} \equiv \mu_\nu$ $(\alpha = e, \mu, \tau)$.

Using these approximations, we obtain the evolution equations for temperature and chemical potential as [35]:[4]

$$\frac{dT_\nu}{dt} = \left(\frac{\partial n_\nu}{\partial \mu_\nu}\frac{\partial \rho_\nu}{\partial T_\nu} - \frac{\partial n_\nu}{\partial T_\nu}\frac{\partial \rho_\nu}{\partial \mu_\nu}\right)^{-1}\left[-3H\left((\rho_\nu + P_\nu)\frac{\partial n_\nu}{\partial \mu_\nu} - n_\nu \frac{\partial \rho_\nu}{\partial \mu_\nu}\right) + \frac{\partial n_\nu}{\partial \mu_\nu}\frac{\delta \rho_\nu}{\delta t} - \frac{\partial \rho_\nu}{\partial \mu_\nu}\frac{\delta n_\nu}{\delta t}\right], \tag{16}$$

$$\frac{d\mu_\nu}{dt} = -\left(\frac{\partial n_\nu}{\partial \mu_\nu}\frac{\partial \rho_\nu}{\partial T_\nu} - \frac{\partial n_\nu}{\partial T_\nu}\frac{\partial \rho_\nu}{\partial \mu_\nu}\right)^{-1}\left[-3H\left((\rho_\nu + P_\nu)\frac{\partial n_\nu}{\partial T_\nu} - n_\nu \frac{\partial \rho_\nu}{\partial T_\nu}\right) + \frac{\partial n_\nu}{\partial T_\nu}\frac{\delta \rho_\nu}{\delta t} - \frac{\partial \rho_\nu}{\partial T_\nu}\frac{\delta n_\nu}{\delta t}\right], \tag{17}$$

$$\frac{dT_\phi}{dt} = \left(\frac{\partial n_\phi}{\partial \mu_\phi}\frac{\partial \rho_\phi}{\partial T_\phi} - \frac{\partial n_\phi}{\partial T_\phi}\frac{\partial \rho_\phi}{\partial \mu_\phi}\right)^{-1}\left[-3H\left((\rho_\phi + P_\phi)\frac{\partial n_\phi}{\partial \mu_\phi} - n_\phi \frac{\partial \rho_\phi}{\partial \mu_\phi}\right) + \frac{\partial n_\phi}{\partial \mu_\phi}\frac{\delta \rho_\phi}{\delta t} - \frac{\partial \rho_\phi}{\partial \mu_\phi}\frac{\delta n_\phi}{\delta t}\right], \tag{18}$$

$$\frac{d\mu_\phi}{dt} = -\left(\frac{\partial n_\phi}{\partial \mu_\phi}\frac{\partial \rho_\phi}{\partial T_\phi} - \frac{\partial n_\phi}{\partial T_\phi}\frac{\partial \rho_\phi}{\partial \mu_\phi}\right)^{-1}\left[-3H\left((\rho_\phi + P_\phi)\frac{\partial n_\phi}{\partial T_\phi} - n_\phi \frac{\partial \rho_\phi}{\partial T_\phi}\right) + \frac{\partial n_\phi}{\partial T_\phi}\frac{\delta \rho_\phi}{\delta t} - \frac{\partial \rho_\phi}{\partial T_\phi}\frac{\delta n_\phi}{\delta t}\right], \tag{19}$$

$$\frac{dT_\gamma}{dt} = -HT_\gamma, \tag{20}$$

with n_i being the number density of particle i. The number and energy density transfer rate of neutrinos are given by

$$\frac{\delta n_\nu}{\delta t} = \sum_\alpha \left(\frac{\delta n_{\nu_\alpha}}{\delta t} + \frac{\delta n_{\bar{\nu}_\alpha}}{\delta t}\right), \tag{21}$$

$$\frac{\delta \rho_\nu}{\delta t} = \sum_\alpha \left(\frac{\delta \rho_{\nu_\alpha}}{\delta t} + \frac{\delta \rho_{\bar{\nu}_\alpha}}{\delta t}\right). \tag{22}$$

Since ϕ and ν are no longer strongly coupled to the photon in this period, their chemical potentials are no longer guaranteed to be zero. Thus, the above evolution equations for μ_ν and μ_ϕ are indispensable.

[4] A derivation of these equations can be found in Appendix A.

3.3. *Calculation of the number and energy transfer rates*

To solve the evolution equations for temperatures and chemical potentials, we need to calculate the number and the energy transfer rates. For processes $\phi \leftrightarrow \nu_\alpha \nu_\beta$ and $\phi \leftrightarrow \bar{\nu}_\alpha \bar{\nu}_\beta$, the number and the energy transfer rate of ϕ are described as follows [35]:

$$\left.\frac{\delta n_\phi}{\delta t}\right|_{\phi\leftrightarrow\nu_\alpha\nu_\beta} = \left.\frac{\delta n_\phi}{\delta t}\right|_{\phi\leftrightarrow\bar{\nu}_\alpha\bar{\nu}_\beta} = \frac{m_\phi^2\Gamma_{\phi\to\nu_\alpha\nu_\beta}}{2\pi^2}\left[T_\nu e^{2\mu_\nu/T_\nu}K_1\left(\frac{m_\phi}{T_\nu}\right) - T_\phi e^{\mu_\phi/T_\phi}K_1\left(\frac{m_\phi}{T_\phi}\right)\right], \tag{23}$$

$$\left.\frac{\delta \rho_\phi}{\delta t}\right|_{\phi\leftrightarrow\nu_\alpha\nu_\beta} = \left.\frac{\delta \rho_\phi}{\delta t}\right|_{\phi\leftrightarrow\bar{\nu}_\alpha\bar{\nu}_\beta} = \frac{m_\phi^3\Gamma_{\phi\to\nu_\alpha\nu_\beta}}{2\pi^2}\left[T_\nu e^{2\mu_\nu/T_\nu}K_2\left(\frac{m_\phi}{T_\nu}\right) - T_\phi e^{\mu_\phi/T_\phi}K_2\left(\frac{m_\phi}{T_\phi}\right)\right]. \tag{24}$$

Actually, in addition to the decay and inverse decay of ϕ, there also exist the scattering and the annihilation processes of the Majoron. However, we neglect these processes because we assume $|g_{\alpha\beta}| \lesssim 10^{-7}$, as mentioned at the beginning of this section. In this case, the number transfer rate for ϕ is given by

$$\begin{aligned}\frac{\delta n_\phi}{\delta t} &= \sum_{\alpha\le\beta}\left(\left.\frac{\delta n_\phi}{\delta t}\right|_{\phi\leftrightarrow\nu_\alpha\nu_\beta} + \left.\frac{\delta n_\phi}{\delta t}\right|_{\phi\leftrightarrow\bar{\nu}_\alpha\bar{\nu}_\beta}\right) \\ &= \frac{m_\phi^2\Gamma_\phi}{2\pi^2}\left[T_\nu e^{2\mu_\nu/T_\nu}K_1\left(\frac{m_\phi}{T_\nu}\right) - T_\phi e^{\mu_\phi/T_\phi}K_1\left(\frac{m_\phi}{T_\phi}\right)\right],\end{aligned} \tag{25}$$

where Γ_ϕ is the total decay width of ϕ, given by

$$\Gamma_\phi \equiv \sum_{\alpha\le\beta}(\Gamma_{\phi\to\nu_\alpha\nu_\beta} + \Gamma_{\phi\to\bar{\nu}_\alpha\bar{\nu}_\beta}) = \frac{m_\phi\lambda^2}{4\pi}, \tag{26}$$

where $\lambda^2 \equiv \mathrm{tr}(g^\dagger g)$. In the same way, the energy transfer rate for ϕ is written as

$$\begin{aligned}\frac{\delta \rho_\phi}{\delta t} &= \sum_{\alpha\le\beta}\left(\left.\frac{\delta \rho_\phi}{\delta t}\right|_{\phi\leftrightarrow\nu_\alpha\nu_\beta} + \left.\frac{\delta \rho_\phi}{\delta t}\right|_{\phi\leftrightarrow\bar{\nu}_\alpha\bar{\nu}_\beta}\right) \\ &= \frac{m_\phi^3\Gamma_\phi}{2\pi^2}\left[T_\nu e^{2\mu_\nu/T_\nu}K_2\left(\frac{m_\phi}{T_\nu}\right) - T_\phi e^{\mu_\phi/T_\phi}K_2\left(\frac{m_\phi}{T_\phi}\right)\right].\end{aligned} \tag{27}$$

The transfer rates for neutrinos, $\delta n_\nu/\delta t$ and $\delta\rho_\nu/\delta t$, can be obtained from the number and the energy conservation law. In the present case, the physics does not depend on a basis of neutrinos, because the neutrino masses are neglected. This is understood from the fact that Γ_ϕ depends on $g_{\alpha\beta}$ only in the form $\mathrm{tr}(g^\dagger g)$. Thus, without loss of generality, we can assume that $g_{\alpha\beta}$ has only diagonal components, and the number conservation is expressed as

$$\left.\frac{\delta n_{\nu_\alpha}}{\delta t}\right|_{\phi\leftrightarrow\nu_\alpha\nu_\alpha} = -2\left.\frac{\delta n_\phi}{\delta t}\right|_{\phi\leftrightarrow\nu_\alpha\nu_\alpha}, \tag{28}$$

which leads to

$$\frac{\delta n_\nu}{\delta t} = \sum_\alpha\left(\left.\frac{\delta n_{\nu_\alpha}}{\delta t}\right|_{\phi\leftrightarrow\nu_\alpha\nu_\alpha} + \left.\frac{\delta n_{\bar{\nu}_\alpha}}{\delta t}\right|_{\phi\leftrightarrow\bar{\nu}_\alpha\bar{\nu}_\alpha}\right) = -2\frac{\delta n_\phi}{\delta t}. \tag{29}$$

On the other hand, energy conservation leads to

$$\left.\frac{\delta \rho_{\nu_\alpha}}{\delta t}\right|_{\phi\leftrightarrow\nu_\alpha\nu_\alpha} = -\left.\frac{\delta \rho_\phi}{\delta t}\right|_{\phi\leftrightarrow\nu_\alpha\nu_\alpha}. \tag{30}$$

From Eq. (30), $\delta\rho_\nu/\delta t$ is found to be

$$\frac{\delta\rho_\nu}{\delta t} = \sum_\alpha \left(\frac{\delta\rho_{\nu_\alpha}}{\delta t}\bigg|_{\phi\leftrightarrow\nu_\alpha\nu_\alpha} + \frac{\delta\rho_{\bar{\nu}_\alpha}}{\delta t}\bigg|_{\phi\leftrightarrow\bar{\nu}_\alpha\bar{\nu}_\alpha} \right) = -\frac{\delta\rho_\phi}{\delta t}. \tag{31}$$

4. Numerical calculation

In this section we discuss the initial conditions and the parameters for the evolution equations of temperatures and the chemical potentials derived in the previous section, and show the numerical results. The software used for the calculations is partially based on `NUDEC_BSM` [35].

4.1. Initial conditions and integration range

Before $e^\pm$ annihilation We solve the system of differential equations in Eqs. (11) and (12) starting from $T_\gamma = T_\nu = 20\,\mathrm{MeV}$, at which all the particles are in thermal equilibrium, to $T_\gamma \sim 10^{-2}\,\mathrm{MeV}$, where the $e^\pm$ annihilation has taken place.

After $e^\pm$ annihilation Let us consider solving the system of differential equations in Eqs. (16)–(20) from the temperature where the Majoron hardly exists. To see when the Majoron can be produced in the early universe, we can consider $\langle\Gamma_{\nu\nu\to\phi}\rangle/H$, where $\langle\Gamma_{\nu\nu\to\phi}\rangle$ is the thermally averaged neutrino inverse decay rate, and H is the Hubble rate. The ratio $\langle\Gamma_{\nu\nu\to\phi}\rangle/H$ is written as [35]

$$\frac{\langle\Gamma_{\nu\nu\to\phi}\rangle}{H} = \frac{1}{81K_1(3)}\Gamma_{\mathrm{eff}}\left(\frac{m_\phi}{T_\nu}\right)^4 K_1\left(\frac{m_\phi}{T_\nu}\right), \tag{32}$$

$$\Gamma_{\mathrm{eff}} \equiv \frac{\langle\Gamma_{\nu\nu\to\phi}\rangle}{H}\bigg|_{T_\nu=m_\phi/3} \simeq \left(\frac{\lambda}{4\times10^{-12}}\right)^2\left(\frac{\mathrm{keV}}{m_\phi}\right). \tag{33}$$

This is illustrated in [35, Fig. 2]. Imposing $\langle\Gamma_{\nu\nu\to\phi}\rangle/H < 10^{-4}$, we obtain the condition for T_ν as follows:

$$\frac{T_\nu}{m_\phi} > \left(\frac{\Gamma_{\mathrm{eff}}}{81K_1(3)\times10^{-4}}\right)^{1/3} \simeq 10\,\Gamma_{\mathrm{eff}}^{1/3}. \tag{34}$$

Here, we use the approximation $K_1(x) \sim 1/x$ for $x < 1$, because the situation with $T_\nu/m_\phi > 1$ is what we want to consider. If we set the range $\Gamma_{\mathrm{eff}} \leq 10^3$, the initial value of T_ν should satisfy $T_\nu \gtrsim 100 m_\phi$. Thus, we will take

$$T_\nu = 100\,m_\phi \tag{35}$$

as the initial condition for T_ν. As the initial condition for T_γ/T_ν, we use the numerical values after $e^\pm$ annihilation ($T_\gamma \simeq 10^{-2}\,\mathrm{MeV}$) obtained by solving Eqs. (11) and (12).

The remaining initial conditions are determined so that $\rho_\phi/\rho_\nu < 10^{-12}$ is satisfied. Since the Majoron is ultra-relativistic for $T_\nu = 100\,m_\phi$, we can treat the Majoron as a massless particle, so ρ_ϕ/ρ_ν is written as

$$\frac{\rho_\phi}{\rho_\nu} = \frac{1}{6}\left(\frac{T_\phi}{T_\nu}\right)^4 \frac{\mathrm{Li}_4(e^{\mu_\phi/T_\phi})}{-\mathrm{Li}_4(-e^{\mu_\nu/T_\nu})} = \frac{4}{21}\left(\frac{T_\phi}{T_\nu}\right)^4\left(1 + a\frac{\mu_\phi}{T_\phi} - \frac{6}{7}a\frac{\mu_\nu}{T_\nu} + \cdots\right). \tag{36}$$

Here, $\mathrm{Li}_s(z)$ is the polylogarithm and $a \equiv \zeta(3)/\zeta(4) \sim 1.2/1.08 \sim 1.1$. Therefore, to satisfy $\rho_\phi/\rho_\nu < 10^{-12}$, the parameters should be

$$\frac{T_\phi}{T_\nu} \lesssim 10^{-3}, \qquad \left|\frac{\mu_\phi}{T_\phi}\right| < 1, \qquad \left|\frac{\mu_\nu}{T_\nu}\right| < 1. \tag{37}$$

This means that the condition for μ_ϕ is

$$\left|\frac{\mu_\phi}{T_\nu}\right| = \left|\frac{\mu_\phi}{T_\phi}\right| \frac{T_\phi}{T_\nu} < \frac{T_\phi}{T_\nu} \lesssim 10^{-3}. \tag{38}$$

Furthermore, since the Majoron is a boson, μ_ϕ must satisfy

$$\frac{\mu_\phi}{T_\nu} < \frac{m_\phi}{T_\nu} = 10^{-2}, \tag{39}$$

from $\mu_\phi \leq m_\phi$. Here, the equality sign is removed because Bose–Einstein condensation cannot occur due to the very small number density of the Majoron.

As for the initial conditions that satisfy Eqs. (37)–(39), in this paper we take them as

$$\frac{T_\phi}{T_\nu} = 10^{-3}, \qquad \frac{\mu_\nu}{T_\nu} = -10^{-4}, \qquad \frac{\mu_\phi}{T_\nu} = -10^{-5}, \tag{40}$$

according to Ref. [35]. The differential equations are solved until $\rho_\phi/\rho_\nu < 10^{-6}$, when the Majoron has completely decayed away.[5]

4.2. *Parameters*

As mentioned before, we consider the case where the Majoron does not exist in the very early universe and is created after $e^\pm$ annihilation ($T_\gamma \lesssim 10^{-2}$ MeV). To realize this situation, the parameters of the Majoron must satisfy the following conditions:

- Majoron production is most active after $e^\pm$ annihilation.
- Shortly after $e^\pm$ have annihilated ($T_\gamma \simeq 10^{-2}$ MeV), Majoron production is not yet effective.

Since $\langle\Gamma_{\nu\nu\to\phi}\rangle/H$ is maximal when $T_\nu \simeq m_\phi/3$ [35], the above conditions are expressed as

$$m_\phi/3 < 10^{-2}\,\mathrm{MeV}, \qquad \left.\frac{\langle\Gamma_{\nu\nu\to\phi}\rangle}{H}\right|_{T_\nu = 10^{-2}\,\mathrm{MeV}} < 1. \tag{41}$$

4.3. *Results*

Here, we show the results of solving the evolution equations derived in the previous section. In this study the deviation of N_{eff} from the standard value occurs twice, namely before and after the $e^\pm$ annihilation. Thus, it is convenient to write N_{eff} as

$$N_{\mathrm{eff}} = N'_{\mathrm{eff}} + \Delta N'_{\mathrm{eff}}. \tag{42}$$

[5] For $\Gamma_{\mathrm{eff}} < 0.1$, we solve the equations until $\rho_\phi/\rho_\nu < 10^{-7}$ because it takes a long time for the Majoron to decay.

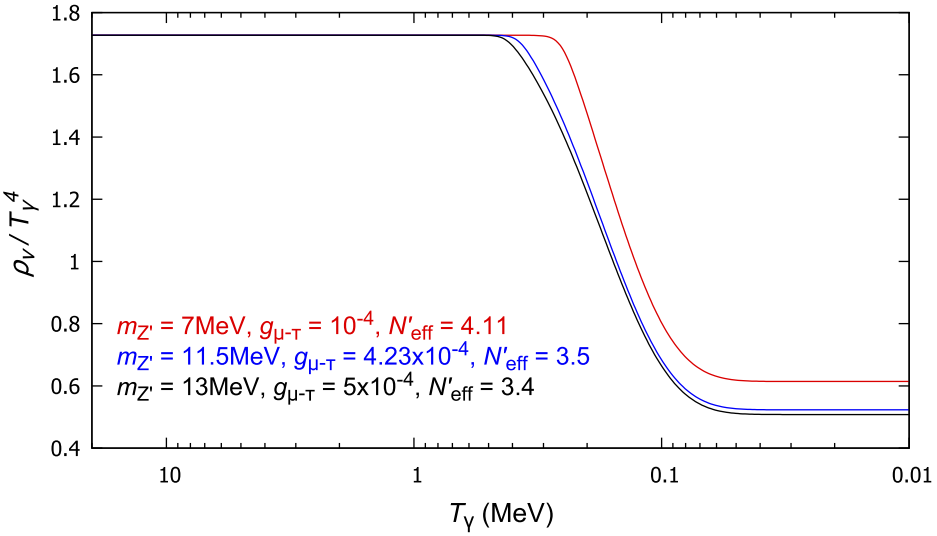

Fig. 2. The evolution of the neutrino energy density for some Z' parameter.

Here, $N'_{\rm eff}$ describes the effective number of neutrino species determined at $T_\nu/T_\gamma =$ constant soon after $e^\pm$ annihilation, and is defined as

$$N'_{\rm eff} = 3\left(\frac{11}{4}\right)^{4/3}\left(\frac{T_\nu}{T_\gamma}\right)^4\Bigg|_{T_\gamma \simeq 10^{-2}\,\rm MeV}. \tag{43}$$

On the other hand, $\Delta N'_{\rm eff}$ represents the change in the effective number of neutrino species due to the Majoron production after $e^\pm$ annihilation. As we will see later, $N'_{\rm eff}$ and $\Delta N'_{\rm eff}$ are not completely independent, and $\Delta N'_{\rm eff}$ slightly depends on $N'_{\rm eff}$.

Figure 2 shows the evolution of the neutrino temperature obtained by solving Eqs. (11) and (12). As can be seen from this figure, the value of $N_{\rm eff}$ is slightly larger than that of the SM $N_{\rm eff}^{\rm SM} \simeq 3.045$ [36,37] due to the new gauge boson Z'.

Figure 3 shows the evolution of the neutrino energy density and the Majoron energy density for the case of $N'_{\rm eff} = 3.5$. This figure shows that for $\Gamma_{\rm eff} \gtrsim 1$, the Majoron begins to be produced by $\nu\nu \to \phi$ when the temperature reaches $T_\nu \gtrsim m_\phi$. After that, the neutrinos and Majoron gradually reach thermal equilibrium. This corresponds to the gently sloping area around the peak in the Figure 3. Since the net energy transfer due to $\phi \leftrightarrow \nu\nu$ is negligibly small, the evolution of the energy densities can be determined by the following Boltzmann equations:

$$\frac{d\rho_\nu}{dt} + 4H\rho_\nu = 0, \tag{44}$$

$$\frac{d\rho_\phi}{dt} + 3H(\rho_\phi + P_\phi) = 0. \tag{45}$$

At temperature $T_\nu \lesssim m_\phi$ the Majoron becomes non-relativistic and ρ_ϕ becomes much larger than P_ϕ. Consequently, the energy densities are derived as

$$\rho_\nu \propto R^{-4}, \qquad \rho_\phi \propto R^{-3}, \tag{46}$$

where R is the scale factor. Therefore, the difference between ρ_ν and ρ_ϕ occurs as the universe expands. At temperature $T_\nu \simeq m_\phi/3$, Majorons start to decay into neutrinos. Since the neutrinos

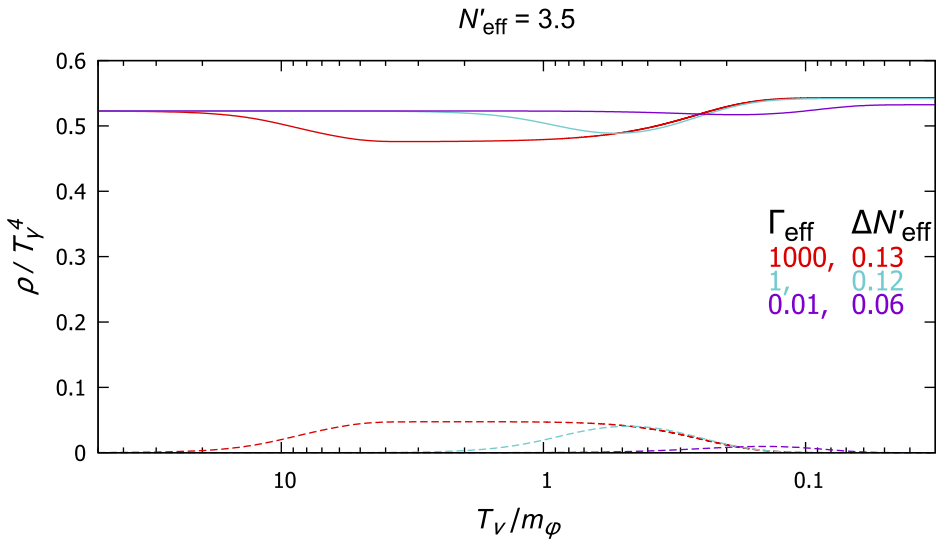

Fig. 3. The evolution of neutrino (solid line) and Majoron (dashed line) energy density for the case of $N'_{\rm eff} = 3.5$.

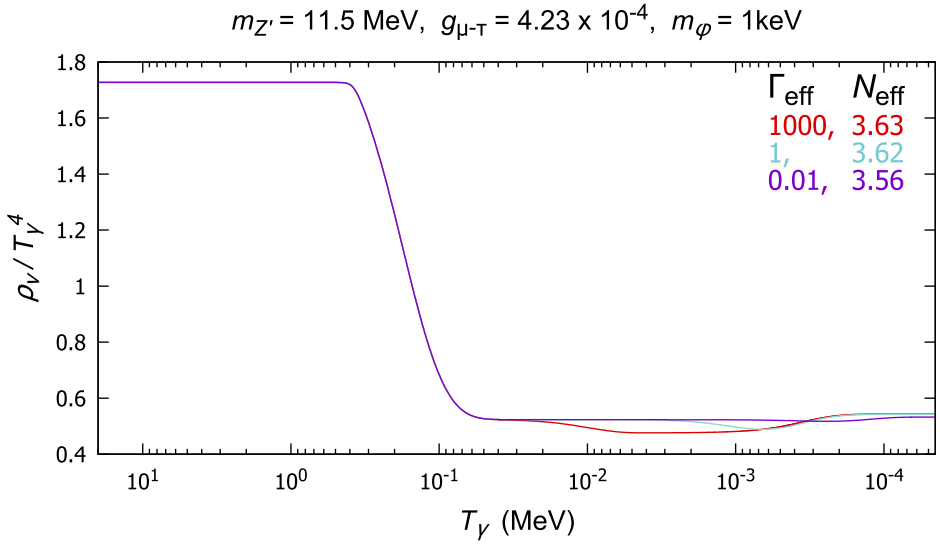

Fig. 4. The evolution of the neutrino energy density for the case of $N'_{\rm eff} = 3.5$, $m_\phi = 1$ keV.

produced by this decay are more energetic than the existing neutrinos, the overall neutrino energy density slightly increases, resulting in a slightly larger $N_{\rm eff}$.

Figure 4 shows the evolution of the neutrino energy density for the case of $N'_{\rm eff} = 3.5, m_\phi = 1$ keV. This figure is obtained by smoothly connecting Figs. 2 and 3 at $T_\gamma \simeq 10^{-2}$ MeV.

Figure 5 shows the $\Gamma_{\rm eff}$ dependence of $\Delta N'_{\rm eff}$ for some $N'_{\rm eff}$. The parameters $\Delta N'_{\rm eff}$ and $N'_{\rm eff}$ are not completely independent, and $\Delta N'_{\rm eff}$ slightly depends on $N'_{\rm eff}$. As you can see, $\Delta N'_{\rm eff}$ becomes larger for larger $N'_{\rm eff}$; the reason is as follows: A large $N'_{\rm eff}$ corresponds to a large number of neutrinos after $e^\pm$ annihilation. For $\Gamma_{\rm eff} \gtrsim 1$, which corresponds to the case where the thermal equilibrium between the Majoron and neutrino is reached due to $\phi \leftrightarrow \nu\nu$, this process acts to equalize the number of neutrinos and Majorons. Thus, for a larger number of neutrinos after $e^\pm$ annihilation, more neutrinos are converted to Majorons. As a result, the neutrino energy density at $T_\nu \ll m_\phi$ becomes larger,

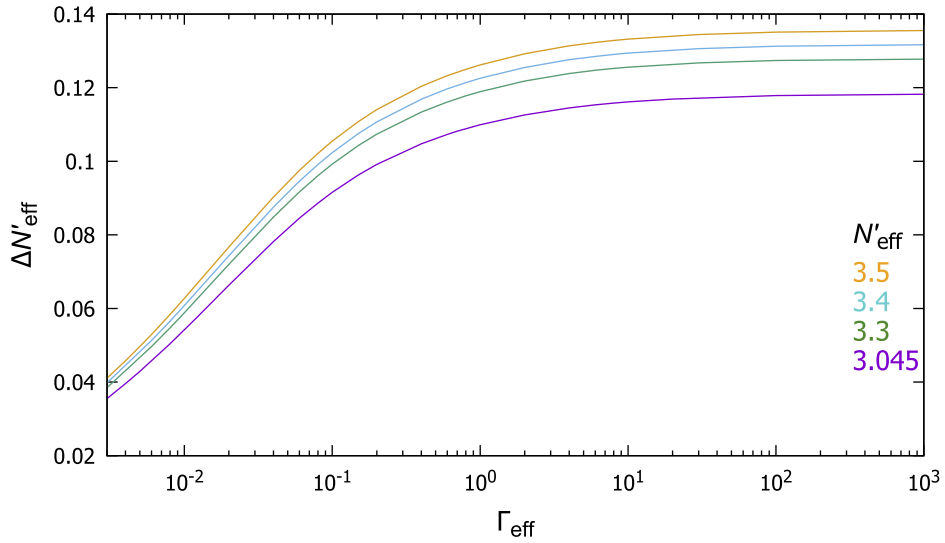

Fig. 5. The $\Gamma_{\rm eff}$ dependence of $\Delta N'_{\rm eff}$ for some $N'_{\rm eff}$.

yielding an increase in $\Delta N'_{\rm eff}$. On the other hand, for $\Gamma_{\rm eff} \ll 1$, thermal equilibrium is not achieved between ν and ϕ, but a small number of Majorons are produced by $\nu\nu \to \phi$. This process occurs more often for a larger number of neutrinos after $e^{\pm}$ annihilation. Thus, the production of Majorons increases slightly and leads to an increase in $\Delta N'_{\rm eff}$. Note that the contribution of the Majoron $\Delta N'_{\rm eff}$ cannot be larger than ~ 0.12 in the case of the SM $N'_{\rm eff} = 3.045$.

Using $N'_{\rm eff}$ and $\Delta N'_{\rm eff}$ defined above, we can write $N_{\rm eff}$ as in Eq. (42). If we fix either $N'_{\rm eff}$ or $\Delta N'_{\rm eff}$, a constraint can be imposed on the other parameter by using the constraint from Planck 2018: $N_{\rm eff} = 3.27 \pm 0.15$ with 68% C.L. [11]. Although various patterns are possible, we will only discuss the following two cases.

$N'_{\rm eff} \simeq 3.4$: Figure 6 shows the parameter space of the Majoron in the presence of Z' that realizes $N'_{\rm eff} = 3.4$. The solid and dotted blue lines are the contour lines of $\Delta N'_{\rm eff}$ ($\Gamma_{\rm eff}$). The solid and dotted red lines represent the same contour lines without the Z' boson ($N'_{\rm eff} = 3.045$). The area below the dashed purple line corresponds to Eq. (41). The blue region ($\Delta N'_{\rm eff} \lesssim 0.1$) represents the region where the Hubble tension can be resolved ($3.4 \lesssim N_{\rm eff} \lesssim 3.5$). The lower limit of the mass of the Majoron is taken to be 10^{-6} MeV because neutrino masses are not negligible below this value. The upper limit of the Majoron mass (3×10^{-2} MeV) corresponds to the first condition in Eq. (41), $m_\phi/3 < 10^{-2}$ MeV. If the Z' boson is in the parameter region where the $(g-2)_\mu$ anomaly can be solved, the Hubble tension and the $(g-2)_\mu$ anomaly can be resolved simultaneously in the blue region. Furthermore, the gold region above the contour line of $\Delta N'_{\rm eff} = 0.1$ is excluded at more than a $2\,\sigma$ level.

$\Delta N'_{\rm eff} \simeq 0.1$: Figure 7 shows the Z' parameter space near the region where the $(g-2)_\mu$ anomaly can be resolved. The region between the solid and dashed dotted lines ($3.2 \lesssim N'_{\rm eff} \lesssim 3.5$) represents the region where the Hubble tension can be resolved only by the Z' boson, as in previous studies (e.g. [20, Fig. 5]). The region between the dashed and dashed double-dotted lines ($3.1 \lesssim N'_{\rm eff} \lesssim 3.4$) represents the same region in the presence of the Majoron that realizes $\Delta N'_{\rm eff} \simeq 0.1$. In this case, the parameter region where the Hubble tension can be resolved is slightly shifted toward the larger

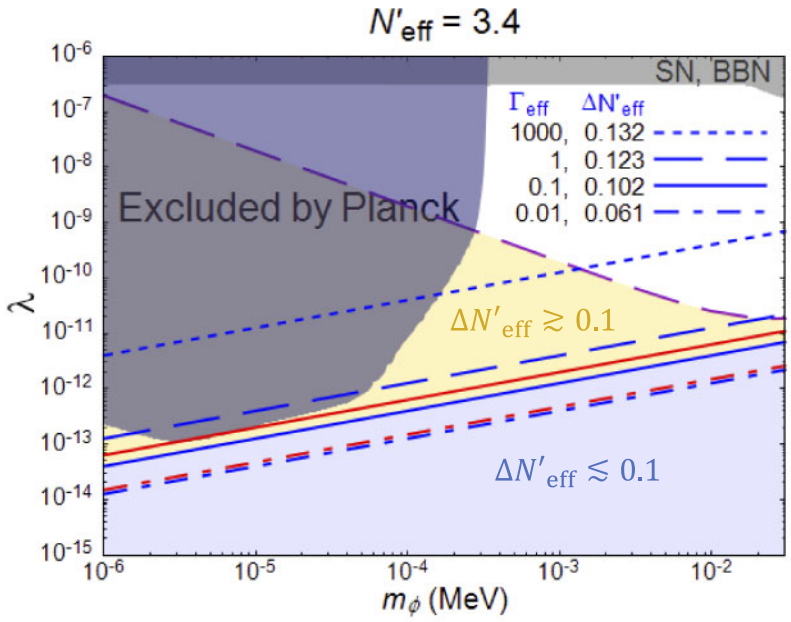

Fig. 6. Parameter space of the Majoron in the presence of Z' that realizes $N'_{\rm eff} = 3.4$. The solid and dotted blue lines are the contour lines of $\Delta N'_{\rm eff}$ ($\Gamma_{\rm eff}$). The solid and dotted red lines represent the same contour lines without the Z' boson ($N'_{\rm eff} = 3.045$). The area below the dashed purple line corresponds to one which satisfies Eq. (41). The gold region represents the region where $\Delta N'_{\rm eff} \gtrsim 0.1$ holds. The blue region represents the parameter region where Hubble tensions can be resolved ($3.4 \lesssim N_{\rm eff} \lesssim 3.5$). The dark blue region is excluded by Planck 2018 data [25]. The gray region is excluded by SN1987A [32,33], BBN [25]. The white region cannot be treated in this paper.

value of $m_{Z'}$. As a result, a new allowed region emerges for larger $m_{Z'}$. The choice of parameters $m_{Z'} \simeq 13 - 26\,\text{MeV}$ and $g_{\mu-\tau} \simeq (3.6\text{–}7) \times 10^{-4}$ can resolve the Hubble tension and $(g-2)_\mu$ anomaly simultaneously in the presence of the Majoron. The region to the left of the $N'_{\rm eff} = 3.4$ contour line is excluded at more than a $2\,\sigma$ level.

5. Summary

We have explored the possibilities of resolving the Hubble tension and $(g-2)_\mu$ anomaly simultaneously in realistic $\text{U}(1)_{L_\mu - L_\tau}$ models that can explain the origin of neutrino mass. In these models, there is a new light gauge boson Z' and a new light scalar, the Majoron ϕ. It arises from the spontaneous breaking of the global $\text{U}(1)_L$ symmetry and weakly couples to neutrinos. The parameters of the Z' boson are set to be $10^{-3} \gtrsim g_{\mu-\tau} \gtrsim 10^{-4}$, $m_{Z'} \simeq 10\,\text{MeV}$, neighborhoods of the region that can resolve the $(g-2)_\mu$ anomaly.

We have only focused on the case where the Majoron does not exist at the beginning of the universe and is created by $\nu\nu \to \phi$ after $e^\pm$ annihilation. In this case, the contributions of Z' and ϕ to the effective number $N_{\rm eff}$ can be calculated independently. Thus, it is convenient to write $N_{\rm eff}$ as $N_{\rm eff} = N'_{\rm eff} + \Delta N'_{\rm eff}$, the sum of the effective number after $e^\pm$ annihilations, $N'_{\rm eff}$, and its change due to the Majoron, $\Delta N'_{\rm eff}$. The effective number $N_{\rm eff}$ is evaluated by the evolution equations of temperatures and the chemical potentials of light particles in each period.

For simplicity, the following two cases were discussed. First, we explored the parameter space of the Majoron in the presence of a Z' that realizes $N'_{\rm eff} = 3.4$. In this case, the Hubble tension can be resolved ($N_{\rm eff} \simeq 3.4$–3.5) in the wide region of the parameter space where $\Delta N'_{\rm eff} \lesssim 0.1$

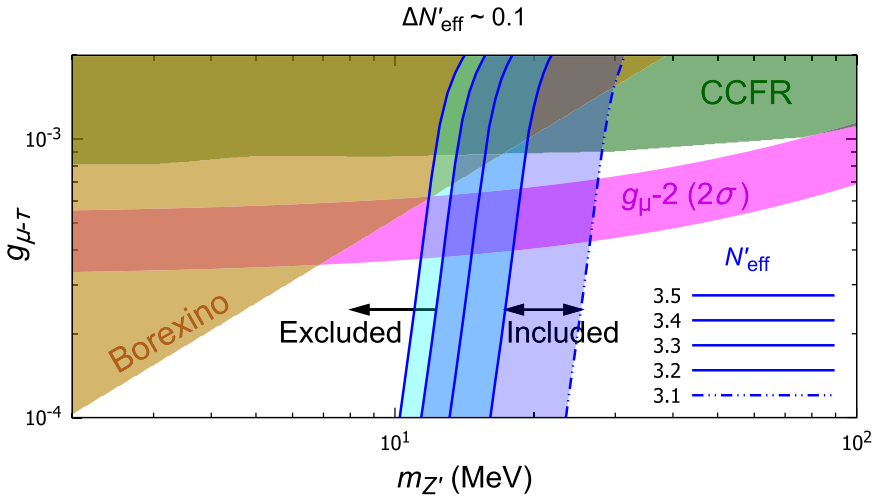

Fig. 7. The Z' parameter space near the region where the $(g-2)_\mu$ anomaly can be resolved. The region between the solid and dashed dotted lines ($3.2 \lesssim N'_{\rm eff} \lesssim 3.5$) represents the region where the Hubble tension can be resolved only by the Z' boson. The region between the dashed and dashed double-dotted lines ($3.1 \lesssim N'_{\rm eff} \lesssim 3.4$) represents the same region in the presence of the Majoron that realizes $\Delta N'_{\rm eff} \simeq 0.1$. The magenta band represents the region where the $(g-2)_\mu$ anomaly can be resolved within a $2\,\sigma$ level [38]. The brown and green regions are excluded by the Borexino and CCFR experiments, respectively [39].

($\lambda \lesssim 10^{-12}$–$10^{-14}$) holds. On the other hand, the region with $\Delta N'_{\rm eff} \gtrsim 0.1$ is excluded at more than $2\,\sigma$ level. In the second case, we surveyed the parameter region of Z' where the Hubble tension can be resolved in the presence of a Majoron that realizes $\Delta N'_{\rm eff} \simeq 0.1$. The choice of parameters $m_{Z'} \simeq 13$–$26\,\text{MeV}$, $g_{\mu-\tau} \simeq (3.6\text{–}7) \times 10^{-4}$, which corresponds to $N'_{\rm eff} \simeq 3.1$–3.4, can resolve the Hubble tension and $(g-2)_\mu$ anomaly simultaneously. On the other hand, the region with $m_{Z'} \lesssim 10\,\text{MeV}$ is excluded at more than a $2\,\sigma$ level.

As a result, we found that the heavier $m_{Z'}$ results in a smaller $N'_{\rm eff}$ and requires a larger $\Delta N'_{\rm eff}$ to resolve the Hubble tension. Therefore, compared to previous studies, the parameter region where the Hubble tension can be resolved is slightly shifted toward the larger value of $m_{Z'}$. Note that $N'_{\rm eff}$ and $\Delta N'_{\rm eff}$ are not completely independent, and $\Delta N'_{\rm eff}$ slightly depends on $N'_{\rm eff}$.

Finally, the Boltzmann equations with simultaneous contributions from Z' and ϕ are more difficult to solve. We leave this for future work.

Acknowledgements

This work was supported by Japan Society for the Promotion of Science (JSPS) KAKENHI Grants No. JP18H01210 (T. A., J. S., T. S., M. J. S. Y.), No. JP19J13812 (K. A.), No. JP18K03651 (T. S.), No. 20K14459 (M. J. S. Y.), and Ministry of Education, Culture, Sports, Science and Technology (MEXT) KAKENHI Grant No. JP18H05543 (J. S., T. S., M. J. S. Y.).

Funding

Open Access funding: SCOAP[3].

Appendix A. Derivation of the evolution equation after $e^\pm$ annihilation

We derive here the evolution equations in Eqs. (16)–(19) after $e^\pm$ annihilation. First of all, the evolution equations for the temperature T_a and chemical potential μ_a of a particle species a that

follows the thermal equilibrium distribution function are given by [35]

$$\frac{dT_a}{dt} = \left(\frac{\partial n_a}{\partial \mu_a}\frac{\partial \rho_a}{\partial T_a} - \frac{\partial n_a}{\partial T_a}\frac{\partial \rho_a}{\partial \mu_a}\right)^{-1}\left[-3H\left((\rho_a + P_a)\frac{\partial n_a}{\partial \mu_a} - n_a\frac{\partial \rho_a}{\partial \mu_a}\right) + \frac{\partial n_a}{\partial \mu_a}\frac{\delta \rho_a}{\delta t} - \frac{\partial \rho_a}{\partial \mu_a}\frac{\delta n_a}{\delta t}\right], \tag{A.1}$$

$$\frac{d\mu_a}{dt} = -\left(\frac{\partial n_a}{\partial \mu_a}\frac{\partial \rho_a}{\partial T_a} - \frac{\partial n_a}{\partial T_a}\frac{\partial \rho_a}{\partial \mu_a}\right)^{-1}\left[-3H\left((\rho_a + P_a)\frac{\partial n_a}{\partial T_a} - n_a\frac{\partial \rho_a}{\partial T_a}\right) + \frac{\partial n_a}{\partial T_a}\frac{\delta \rho_a}{\delta t} - \frac{\partial \rho_a}{\partial T_a}\frac{\delta n_a}{\delta t}\right]. \tag{A.2}$$

In Eqs. (A.1) and (A.2), n_a, ρ_a, and P_a are the particle number density, energy density, and pressure of particle species a, respectively. From the third approximation at the start of Sect. 3.2 and $T_{\nu_\alpha} = T_{\bar{\nu}_\alpha}$, $\mu_{\nu_\alpha} = \mu_{\bar{\nu}_\alpha}$, Eq. (A.1) for the neutrino and antineutrino leads to

$$\begin{aligned}\frac{dT_\nu}{dt} &= \left(\frac{\partial n_{\nu_\alpha}}{\partial \mu_\nu}\frac{\partial \rho_{\nu_\alpha}}{\partial T_\nu} - \frac{\partial n_{\nu_\alpha}}{\partial T_\nu}\frac{\partial \rho_{\nu_\alpha}}{\partial \mu_\nu}\right)^{-1} \\ &\quad\times\left[-3H\left((\rho_{\nu_\alpha} + P_{\nu_\alpha})\frac{\partial n_{\nu_\alpha}}{\partial \mu_\nu} - n_{\nu_\alpha}\frac{\partial \rho_{\nu_\alpha}}{\partial \mu_\nu}\right) + \frac{\partial n_{\nu_\alpha}}{\partial \mu_\nu}\frac{\delta \rho_{\nu_\alpha}}{\delta t} - \frac{\partial \rho_{\nu_\alpha}}{\partial \mu_\nu}\frac{\delta n_{\nu_\alpha}}{\delta t}\right],\end{aligned} \tag{A.3}$$

$$\begin{aligned}\frac{dT_\nu}{dt} &= \left(\frac{\partial n_{\bar{\nu}_\alpha}}{\partial \mu_\nu}\frac{\partial \rho_{\bar{\nu}_\alpha}}{\partial T_\nu} - \frac{\partial n_{\bar{\nu}_\alpha}}{\partial T_\nu}\frac{\partial \rho_{\bar{\nu}_\alpha}}{\partial \mu_\nu}\right)^{-1} \\ &\quad\times\left[-3H\left((\rho_{\bar{\nu}_\alpha} + P_{\bar{\nu}_\alpha})\frac{\partial n_{\bar{\nu}_\alpha}}{\partial \mu_\nu} - n_{\bar{\nu}_\alpha}\frac{\partial \rho_{\bar{\nu}_\alpha}}{\partial \mu_\nu}\right) + \frac{\partial n_{\bar{\nu}_\alpha}}{\partial \mu_\nu}\frac{\delta \rho_{\bar{\nu}_\alpha}}{\delta t} - \frac{\partial \rho_{\bar{\nu}_\alpha}}{\partial \mu_\nu}\frac{\delta n_{\bar{\nu}_\alpha}}{\delta t}\right].\end{aligned} \tag{A.4}$$

In addition, each thermodynamic quantity for $\{\nu_\alpha\}$, $\{\bar{\nu}_\alpha\}$ is expressed by the particle number density n_ν, the energy density ρ_ν, and the pressure P_ν for the total neutrino:

$$n_{\nu_\alpha} = n_{\bar{\nu}_\alpha} = \frac{1}{6}n_\nu, \tag{A.5}$$

$$\rho_{\nu_\alpha} = \rho_{\bar{\nu}_\alpha} = \frac{1}{6}\rho_\nu, \tag{A.6}$$

$$P_{\nu_\alpha} = P_{\bar{\nu}_\alpha} = \frac{1}{6}P_\nu. \tag{A.7}$$

By adding both sides of Eqs. (A.3) and (A.4), and summing over all flavors, we obtain the evolution equation for T_ν, Eq. (16). The evolution equation for μ_ν, Eq. (17), can also be obtained in the same way.

For the Majoron evolution equation, by using Eqs. (A.1) and (A.2) set to $a = \phi$, we obtain the evolution equations for T_ϕ, Eq. (18), and μ_ϕ, Eq. (19).

References

[1] N. Aghanim et al. [Planck Collaboration], Astron. Astrophys. **641**, A5 (2020).
[2] A. G. Riess et al., Astrophys. J. **855**, 136 (2018).
[3] A. G. Riess et al., Astrophys. J. **861**, 126 (2018).
[4] A. G. Riess, S. Casertano, W. Yuan, L. M. Macri, and D. Scolnic, Astrophys. J. **876**, 85 (2019).
[5] K. C. Wong et al., Mon. Not. Roy. Astron. Soc. **498**, 1420 (2020).
[6] W. L. Freedman et al., Astrophys. J. **882**, 34 (2019) [arXiv:1907.05922 [astro-ph.CO]] [Search INSPIRE].
[7] S. Birrer et al., Astron. Astrophys. **643**, A165 (2020).
[8] G. Efstathiou, Mon. Not. Roy. Astron. Soc. **440**, 1138 (2014).
[9] W. L. Freedman, Nature Astron. **1**, 0121 (2017).

[10] M. M. Ivanov, Y. Ali-Haïmoud, and J. Lesgourgues, Phys. Rev. D **102**, 063515 (2020).
[11] N. Aghanim et al. [Planck Collaboration], Astron. Astrophys. **641**, A6 (2020).
[12] H. Hildebrandt et al., Astron. Astrophys. **633**, A69 (2020).
[13] R. Foot, Mod. Phys. Lett. A **6**, 527 (1991).
[14] X.-G. He, G. C. Joshi, H. Lew, and R. R. Volkas, Phys. Rev. D **43**, R22(R) (1991).
[15] R. Foot, X.-G. He, H. Lew, and R. R. Volkas, Phys. Rev. D **50**, 4571 (1994).
[16] X.-G. He, G. C. Joshi, H. Lew, and R. R. Volkas, Phys. Rev. D **44**, 2118 (1991).
[17] S. N. Gninenko and N. V. Krasnikov, Phys. Lett. B **513**, 119 (2001).
[18] S. Baek, N. G. Deshpande, X.-G. He, and P. Ko, Phys. Rev. D **64**, 055006 (2001).
[19] E. Ma, D. P. Roy, and S. Roy, Phys. Lett. B **525**, 101 (2002).
[20] M. Escudero, D. Hooper, G. Krnjaic, and M. Pierre, J. High Energy Phys. **1903**, 071 (2019).
[21] Y. Chikashige, R. N. Mohapatra, and R. D. Peccei, Phys. Lett. B **98**, 265 (1981).
[22] G. B. Gelmini and M. Roncadelli, Phys. Lett. B **99**, 411 (1981).
[23] H. M. Georgi, S. L. Glashow, and S. Nussinov, Nucl. Phys. B **193**, 297 (1981).
[24] J. Schechter and J. W. F. Valle, Phys. Rev. D **25**, 774 (1982).
[25] M. Escudero and S. J. Witte, Eur. Phys. J. C **80**, 294 (2020).
[26] T. Araki, K. Asai, J. Sato, and T. Shimomura, Phys. Rev. D **100**, 095012 (2019).
[27] T. Araki, F. Kaneko, Y. Konishi, T. Ota, J. Sato, and T. Shimomura, Phys. Rev. D **91**, 037301 (2015).
[28] A. Kamada and H.-B. Yu, Phys. Rev. D **92**, 113004 (2015).
[29] T. Araki, F. Kaneko, T. Ota, J. Sato, and T. Shimomura, Phys. Rev. D **93**, 013014 (2016).
[30] A. DiFranzo and D. Hooper, Phys. Rev. D **92**, 095007 (2015).
[31] A. Gando et al. [KamLAND-Zen Collaboration], Phys. Rev. C **86**, 021601(R) (2012).
[32] M. Kachelriess, R. Tomàs, and J. W. F. Valle, Phys. Rev. D **62**, 023004 (2000).
[33] Y. Farzan, Phys. Rev. D **67**, 073015 (2003).
[34] M. Escudero, J. Cosmol. Astropart. Phys. **1902**, 007 (2019).
[35] M. Escudero Abenza, J. Cosmol. Astropart. Phys. **2005**, 048 (2020).
[36] P. F. de Salas and S. Pastor, J. Cosmol. Astropart. Phys. **1607**, 051 (2016).
[37] K. Akita and M. Yamaguchi, J. Cosmol. Astropart. Phys. **2008**, 012 (2020).
[38] B. Abi et al. [Muon $g-2$ Collaboration] , Phys. Rev. Lett. **126**, 141801 (2021).
[39] T. Araki, S. Hoshino, T. Ota, J. Sato, and T. Shimomura, Phys. Rev. D **95**, 055006 (2017).